Available online at www.sciencedirect.com

SCIENCE DIRECT®

ELSEVIER

International Journal of Solids and Structures 41 (2004) 6925–6936

INTERNATIONAL JOURNAL OF SOLIDS and STRUCTURES

www.elsevier.com/locate/ijsolstr

Nonlinear analysis of a SWCNT over a bundle of nanotubes

Zhiling Li [a], Prasad Dharap [a], Satish Nagarajaiah [a,b,*], Ronald P. Nordgren [a,b], Boris Yakobson [b]

[a] *Civil and Environmental Engineering, Rice University, MS 318, 6100 Main Street, Houston, TX 77005, USA*
[b] *Mechanical Engineering and Material Science, Rice University, MS 318, 6100 Main Street, Houston, TX 77005, USA*

Received 6 December 2003; received in revised form 22 May 2004
Available online 10 July 2004

Abstract

The deformation of a single wall carbon nanotube (SWCNT) interacting with a curved bundle of nanotubes is analyzed. The SWCNT is modeled as a straight elastic inextensible beam based on small deformation. The bundle of nanotubes is assumed rigid and the interaction is due to the van der Waals forces. An analytical solution is obtained using a bilinear approximation to the van der Waals forces. The analytical results are in good agreement with the results of two numerical methods. The results indicate that the SWCNT remains near the curved bundle provided that its curvature is below a critical value. For curvatures above this critical value the SWCNT breaks contact with the curved bundle and nearly returns to its straight position. A parameter study shows that the critical curvature depends on the stiffness of the SWCNT and the absolute minimum energy associated with the van der Waals forces but it is independent of the SWCNT's length in general. An analytical estimate of the critical curvature is developed. The results of this study may be applicable to composites of nanotubes where separation phenomena are suspected to occur.

1. Introduction

Since the discovery (Iijima, 1991) of carbon nanotubes, they have been extensively investigated due to their unique mechanical and electrical properties. Numerous studies have shown that carbon nanotubes exhibit superior mechanical and electrical properties as compared to any other known materials and hold substantial promise as super strong fibers for composite. Recent studies have shown the use of nanotubes as actuator (Baughman et al., 1999), sensor (Collins et al., 2000), nanotweezers (Akita et al., 2001) and nanoswitch (Dequesnes et al., 2002). Studies have shown that it is very difficult to disperse carbon nanotubes evenly in a matrix composite. Generally nanotubes form clusters and are found in bundles in composites.

* Corresponding author. Address: Civil and Environmental Engineering, Mechanical Engineering and Material Science, Rice University, MS 318, 6100 Main Street, Houston, TX 77005, USA. Tel.: +1-713-3486207; fax: +1-713-3485268.
E-mail address: nagaraja@rice.edu (S. Nagarajaiah).

0020-7683/$ - see front matter
doi:10.1016/j.ijsolstr.2004.05.043

Nomenclature

EI	the bending stiffness of nanobeam
$y(x)$	the deformation of the nanobeam in fixed coordinate
$r(x)$	the relative deformation, defined by the distance between the center of the nanobeam in the deformed position and the equilibrium position where the van der Waals force is zero
$F(r)$	van der Waals forces between the nanobeam and the substrate
U_0	the minimum energy in the Lennard–Jones energy potential
$U_{\text{Lin}}(r)$	the approximate van der Waals energy
r_s	the distance between the bottom of the nanobeam and top of the substrate when van der Waals force is zero
r_0	the equilibrium distance between the nanobeam and the substrate where the van der Waals force is zero ($r_0 = r_s + d$)
d	the diameter of the nanobeam
k_1	the tangent stiffness of the van der Waals forcing function where the van der Waals force is zero
k_2	the stiffness of the second linear segment in bilinear model
b_2	the interception of the second linear segment in bilinear model
m_{cr}	the critical curvature of the substrate for the jump phenomenon to occur in the nanobeam
m^*	the critical curvature of the substrate for the jump phenomenon to occur in the nanobeam, when the van der Waals forcing function is replaced by linear approximation
L	half length of the nanobeam

Electronic transport through carbon nanotubes is generally discussed in terms of the idealized geometry of free nanotubes unperturbed by interaction with the matrix. But the carbon nanotubes interact with surrounding material through van der Waals forces which are likely responsible for irregularities in the electronic transport properties of adsorbed nanotubes (Hertel et al., 1998; Peng and Cho, 2000). Normally the molecular dynamics (MD) method is applied to simulate the deformation of nanotubes influenced by van der Waals forces. But the MD method needs to consider all the atoms forming the nanotubes. Also, the time step required for a stable integration is very small; this leads to extremely slow convergence for larger systems. Therefore a continuous elastic beam model is adopted in this paper to model and study the behavior of a SWCNT.

The problem considered in this study is the nonlinear interaction and resulting relative deformation between a SWCNT and a substrate consisting of a bundle of SWCNTs with only van der Waals forces interacting between them. Since a bundle of SWCNTs is much stiffer than a SWCNT, it is assumed that the substrate of SWCNTs is rigid. Fig. 1(a) shows the SWCNT near the rigid substrate (model 1) and Fig. 1(b) shows the SWCNT separated from the substrate (model 2). The transfer from model 1 to model 2, called ‘‘jump phenomenon’’, occurs at a critical curvature (Yakobson and Couchman, 2003).

The main objective of this study is to understand the jump phenomenon in detail. Analysis is carried out to determine the critical curvature and the corresponding deformed configuration of the nanotube. Also the influence of the length, the diameter, and the bending stiffness of the nanotube, as well as the van der Waals forcing function, on the critical curvature for jump phenomenon is explored in this study. An analytical method using bilinear approximation of the van der Waals forces is developed. Also the finite element method and shooting method with accurate van der Waals forces are used to study the relative deformation of the nanotube. Good agreement is found in the results of the three methods.

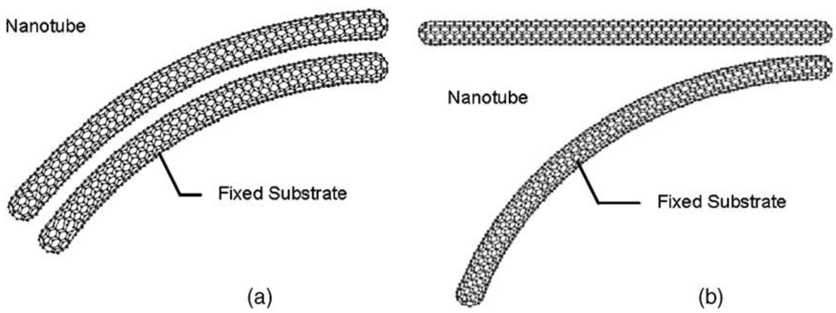

Fig. 1. The deformation of nanotube: (a) Substrate curvature less than the critical curvature; (b) substrate curvature greater than the critical curvature.

2. Beam model

The nanotube is idealized as a straight elastic inextensible beam that in the reference position has the same curvature as that of the fixed substrate and has a uniform offset $r_0 = r_s + d$ from the substrate as shown in Fig. 2, which is the equilibrium position for this nanobeam where zero van der Waals forces act, d is the diameter of the nanobeam and r_s is the distance between inner surfaces of two nanotubes shown in Fig. 2. When the nanobeam deforms, there are only van der Waals forces interacting between them. The van der Waals forcing and energy functions are shown in Fig. 3.

Since the nanobeam as well as the substrate is symmetric about y-axis, only half of the nanobeam is analyzed with slope of the beam and the shear force equal to zero at the origin point or apex and with the moment and the shear force equal to zero at free ends as shown in Fig. 2. The analysis is based on small deformation theory. The equilibrium equation of the nanobeam is:

$$\begin{aligned} & EI\frac{\mathrm{d}^4y(x)}{\mathrm{d}x^4} + F(r(x)) = 0 \\ & \text{with boundary condition (b.c.)} \\ & y^{(1)}(0) = 0, \quad y^{(3)}(0) = 0 \\ & y^{(2)}(L) = 0, \quad y^{(3)}(L) = 0 \end{aligned} \tag{1}$$

where $y(x)$ is the deformation of the nanobeam, $y^{(i)}$ is the ith derivative of y with respect to x and $F(r(x))$ is the van der Waals forces between substrate and the nanobeam. EI is the bending stiffness of the nanobeam.

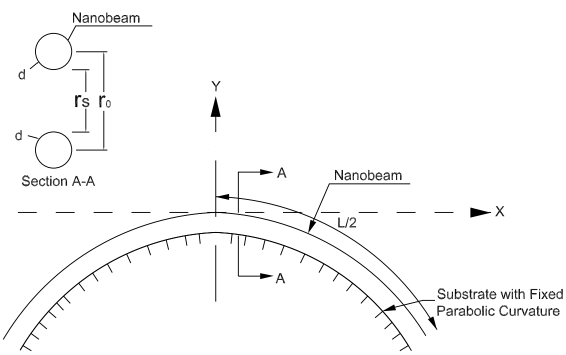

Fig. 2. Initial condition of the nanobeam model.

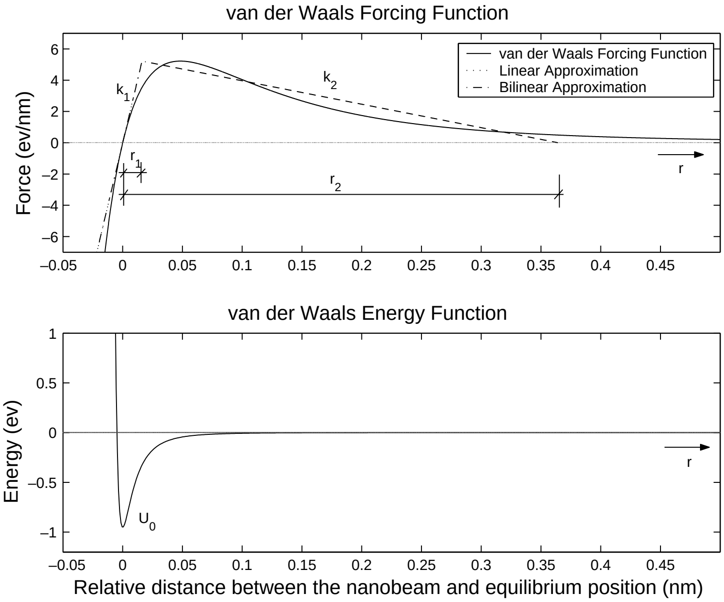

Fig. 3. Van der Waals forcing and energy function.

$r(x) + r_0$ is the relative distance between the nanobeam and the substrate. The curvature of the substrate is parabolic with $Y(x) = mx^2/2$, where m is the curvature of the substrate. Rewriting Eq. (1) with $y(x) = mx^2/2 + r(x) + r_s$:

$$\begin{aligned} & EI\frac{\mathrm{d}^4 r(x)}{\mathrm{d}x^4} + F(r(x)) = 0 \\ & \text{with b.c.} \\ & r^{(1)}(0) = 0, \quad r^{(3)}(0) = 0 \\ & r^{(2)}(L) = -m, \quad r^{(3)}(L) = 0 \end{aligned} \tag{2}$$

The van der Waals force per unit length is expressed as (Israelachvili, 1992):

$$F(r) = 17.81U_0\left[-\left(\frac{3.41}{3.13\frac{r+r_0-d}{r_0-d}+0.28}\right)^{11} + \left(\frac{3.41}{3.13\frac{r+r_0-d}{r_0-d}+0.28}\right)^{5}\right] \tag{3}$$

where U_0 is the minimum energy in the Lennard–Jones energy potential as shown in Fig. 3. r_s is the distance between the surfaces of nanobeam and substrate when van der Waals force is zero. d is the diameter of the nanobeam.

2.1. Analytical solution

2.1.1. Bilinear approximation

Since the van der Waals forcing function is highly nonlinear, it is very difficult to get an exact analytical solution for this problem. Hence the bilinear approximation defined in Eq. (4) is used, instead of the nonlinear van der Waals forcing function, to obtain an analytical solution, i.e.,

$$F(r) = \begin{cases} k_1 r & \text{for } 0 < r < r_1 \\ -k_2 r + b_2 & \text{for } r_1 < r < r_2 \\ 0 & \text{for } r_2 < r < \infty \end{cases} \tag{4}$$

where k_1 is the tangent value of the van der Waals forcing function in Eq. (3) at the point where van der Waals force is zero. Here r_1 is calculated by dividing the maximum attraction force in Eq. (3) by k_1. Also, k_2 and b_2 are obtained by making the area enclosed by the attractive part of the bilinear forcing function with the x axis the same as that of original van der Waals forcing function. Substituting Eq. (4) into Eq. (2) and solving we obtain:

$$r(x) = e^{\lambda_1 x}[A_1 \cos(\lambda_1 x) + A_2 \sin(\lambda_1 x)] + e^{-\lambda_1 x}[A_3 \cos(\lambda_1 x) + A_4 \sin(\lambda_1 x)] \quad \text{for } x < x_1 \tag{5}$$

$$r(x) = B_1 \cos(\lambda_2 x) + B_2 \sin(\lambda_2 x) + B_3 \cosh(\lambda_2 x) + B_4 \sinh(\lambda_2 x) + \frac{b_2}{k_2} \quad \text{for } x_1 < x < x_2 \tag{6}$$

where $\lambda_1 = \sqrt[4]{\frac{k_1}{4EI}}$ and $\lambda_2 = \sqrt[4]{\frac{k_2}{EI}}$. There are a total of 10 unknowns in Eqs. (5) and (6). Boundary conditions provide four equations. Continuity conditions at $x = x_1$ provide four equations. The remaining equations are obtained from constraint conditions: $r = r_1$ at $x = x_1$ and $r = r_2$ at $x = x_2$. Thus there are ten unknown variables and ten equations. Also sine and cosine functions make the problem nonlinear. One way to solve is to search x_1 and x_2 along the length of the nanobeam. It is solved by standard iterative method by first assuming x_1 and x_2 to be known.

2.1.2. Linear approximation

In order to get an analytical expression for the critical curvature for jump phenomenon to occur, an even simpler linear approximation expression is introduced to replace the original van der Waals forcing function, namely:

$$F(r) = \begin{cases} k_1 r & \text{for } r < r_1 \\ 0 & \text{for } r > r_1 \end{cases} \tag{7}$$

where k_1 and r_1 are the same as defined in Eq. (4). Substituting Eq. (7) into Eq. (2):

$$\begin{aligned} &EI\frac{d^4 r(x)}{dx^4} + k_1 r(x) = 0 \text{ for } 0 < x < x_1 \\ &r(x_1) = r_1 \\ &r^{(1)}(0) = 0, \quad r^{(3)}(0) = 0 \\ &M(L) = -mEI, \quad Q(L) = 0 \text{ for small } m \end{aligned} \tag{8}$$

Normally nanotubes have very high aspect ratios (length-to-diameter ratio). The solution for nanobeams with a linear approximation of van der Waals force is derived based on semi-infinite beam on elastic foundation with a concentrated moment $M(L) = -mEI$ on the right hand side of the beam.

$$r(x) = -\frac{m}{2\lambda_1^2} e^{-\lambda_1(L-x)}[\cos(\lambda_1(L-x)) - \sin(\lambda_1(L-x))] \text{ for small } m \tag{9}$$

where $\lambda_1 = \sqrt[4]{\frac{k_1}{4EI}}$. The value of x where $r(x) = 0$ can be calculated by $\cos(\lambda_1(L-x)) - \sin(\lambda_1(L-x)) = 0$, that is, $\lambda_1(L-x) = \frac{\pi}{4}, \frac{5\pi}{4}$, etc. $\left(L_1 = \frac{\pi}{4\lambda_1}, L_2 = \frac{5\pi}{4\lambda_1}\right)$, which is independent of m. Since $r(x)$ is small between 0 and $L - L_2$, the corresponding reaction due to elastic support is neglected, provided $L/L_2 > 2$. When $r(L)$ is equal to r_1 (m will reach m^*), the critical curvature under the linear approximation can be obtained from Eq. (9):

$$m^* = -\sqrt{\frac{k_1 r_1^2}{EI}} \tag{10}$$

From Eq. (10) it can also be observed that m^* does not depend on the length of the nanobeam if the length of beam is long enough, such as $L/L_2 > 2$. It is observed that m^* is proportional to the square root of $k_1 r_1^2$, which is twice the area enclosed by the attraction forces of the linear function has shown in Eq. (7). This term has dimensions of energy, which corresponds to the absolute minimum energy in the energy function defined in Eq. (11).

$$U_{\text{Lin}}(r) = \begin{cases} \frac{k_1 r^2}{2} - \frac{k_1 r_1^2}{2} & r < r_1 \\ 0 & r > r_1 \end{cases} \tag{11}$$

It is assumed that the energy is zero when r approaches infinity. From the analysis in this section it can be seen that the critical curvature is a function of the absolute minimum energy of the van der Waals forcing function and the stiffness of the beam.

2.2. Finite element method (FEM)

FEM is used to calculate the deformations of the nanobeam and the results are compared with the analytical results. Expressing Eq. (2) in Galerkin weak form:

$$\int_{x=0}^{L} \left(EI \frac{\mathrm{d}^2 w(x)}{\mathrm{d}x^2} \frac{\mathrm{d}^2 r(x)}{\mathrm{d}x^2} + w(x) F(r(x)) \right) \mathrm{d}x = -mEI \frac{\mathrm{d}w(x)}{\mathrm{d}x}\bigg|_{x=L} \tag{12}$$

where $w(x)$ is admissible test function. The Newton–Raphson method is used to solve this problem where the van der Waals forcing function is expressed as:

$$F(r) = F(\tilde{r}_0) + \frac{\mathrm{d}}{\mathrm{d}r} F(\tilde{r}_0) \Delta r + O(\Delta r^2) \tag{13}$$

Setting $w = \sum_{A \in \eta_g} C_A \phi_A$, $r = \sum_{B \in \eta} (d_B + \Delta d_B) \phi_B$ and $\Delta r = \sum_{B \in \eta} \Delta d_B \phi_B$, where ϕ is shape function, Δd_B is the unknown variable using which d_B is computed, η_g is the set of all unknown degrees of freedom at nodes in the finite element mesh and η is total number of nodes multiplied by the degrees of freedom at each node. Substituting Eq. (13) into Eq. (12) and using Newton–Raphson method:

$$\begin{aligned} &\sum_{A \in \eta_g} C_A \left[\sum_{B \in \eta} \left(\int_{x=0}^{L} EI \frac{\mathrm{d}^2 \phi_A}{\mathrm{d}x^2} \frac{\mathrm{d}^2 \phi_B}{\mathrm{d}x^2} \mathrm{d}x + \int_{x=0}^{L} \phi_A \frac{\mathrm{d}F(\tilde{r}_0)}{\mathrm{d}r} \phi_B \mathrm{d}x \right) \Delta d_B \right] \\ &\quad = -mEI \frac{\mathrm{d}w(x)}{\mathrm{d}x}\bigg|_{x=L} - \sum_{A \in \eta_g} C_A \left[\int_{x=0}^{L} \phi_A F(\tilde{r}_0) \mathrm{d}x + \sum_{B \in \eta_g} \left(\int_{x=0}^{L} EI \frac{\mathrm{d}^2 \phi_A}{\mathrm{d}x^2} \frac{\mathrm{d}^2 \phi_B}{\mathrm{d}x^2} \mathrm{d}x \right) d_B \right] \end{aligned} \tag{14}$$

Defining

$$K_{AB} = \int_{x=0}^{L} EI \frac{\mathrm{d}^2 \phi_A}{\mathrm{d}x^2} \frac{\mathrm{d}^2 \phi_B}{\mathrm{d}x^2} \mathrm{d}x, \quad K_{AB}^* = \int_{x=0}^{L} \phi_A \frac{\mathrm{d}F(\tilde{r}_0)}{\mathrm{d}r} \phi_B \mathrm{d}x, \quad F_A = \int_{x=0}^{L} \phi_A F(\tilde{r}_0) \mathrm{d}x$$

and rewriting Eq. (14):

$$\sum_{A \in \eta_g} C_A \left[\sum_{B \in \eta} (K_{AB} + K_{AB}^*) \Delta d_B \right] = -mEI \frac{\mathrm{d}w(x)}{\mathrm{d}x}\bigg|_{x=L} - \sum_{A \in \eta_g} C_A \left[\sum_{B \in \eta} K_{AB} d_B + F_A \right] \tag{15}$$

As there are four unknown variables for each element, minimum order of power series shape function for one element should be 3. Hence Hermite interpolation polynomials are used:

$$\begin{aligned} \phi_1^e(x) &= 1 - 3s^2 + 2s^3, \quad \phi_2^e(x) = l^e s(s-1)^2 \\ \phi_3^e(x) &= s^2(3-2s), \quad \phi_4^e(x) = l^e s^2(s-1) \end{aligned} \tag{16}$$

where l^e is the length of one element. $s = \frac{x-x_1}{x_2-x_1}$, here x_1 and x_2 are the left and right coordinates of the element.

Since the forcing function in Eq. (15) is highly nonlinear, the Newton–Raphson method may have convergence difficulties if the initial guess d_B is far away from the solution; hence an incremental load method is used. First the substrate is assumed to be straight with zero curvature and initial solutions for the beam are obtained. The curvature of the substrate, m, is increased and the solution in the previous step is used as an initial guess for this step and the convergent solution for this step is computed. Then m is increased and the above steps are repeated till required m is reached.

2.3. Shooting method

This problem is solved as a two point boundary value problem using the numerical shooting method. Here the unknown deflection $y(0)$ and the curvature $y^{(2)}(0)$ are assumed at the start. After reaching the free end it is checked for zero moment as well as zero shear at the free end. Since the nanobeam is in equilibrium, the summation of forces along the length of the nanobeam must be zero. This additional criterion needs to be satisfied. If all these conditions are not satisfied then a new initial guess is assumed and the procedure is repeated. These conditions can be written in a vector format as

$$\mathbf{F} = \left\{ \begin{array}{l} y^{(2)}(x=L) \\ y^{(3)}(x=L) \\ \sum_{x=0}^{L} f(r(x)) \end{array} \right\} = 0 \tag{17}$$

The Newton–Raphson method provides a systematic way of carrying out iterations. Iterations are carried out till the discrepancy vector $\mathbf{F} = 0$ or is within tolerance limit. For the convergence of the shooting method it is necessary that the initial guess is close enough to the actual solution. Hence to start the shooting method the initial guess for the unknown boundary conditions is obtained from the analytical results.

3. Results and discussions

The stiffness of the nanobeam is calculated by using $EI = \pi C d^3$ ($C = 2152.8$ eV/nm^2 is the in-plane stiffness, based on ab initio calculations (Kudin et al., 2001)), where d is the diameter of the nanobeam. In the following discussion, $r(x)$ is termed as relative deformation.

Deformations of the nanobeam, $y(x)$, for different curvatures of the substrate computed using FEM, analytical method and shooting method, are shown in Fig. 4(a). Also, van der Waals forces for different curvatures of the substrate are compared in Fig. 4(b). Since solution by FEM and shooting method essentially agree it is hard to distinguish the two solutions from Fig. 4. From Figs. 4(a) and (b) it can be observed that FEM results as well as shooting method results are in good agreement with the analytical solution using bilinear approximation. This validates the results by FEM solution. Henceforth, the FEM solution is used. For $L = 20$ nm and $d = 0.40$ nm nanotube, when the curvature of the substrate changes from -0.06 to -0.07 nm^{-1}, the relative deformations of the nanobeam suddenly change from small deformation to significant deformation as shown in Fig. 4(a), which is referred as jump phenomenon

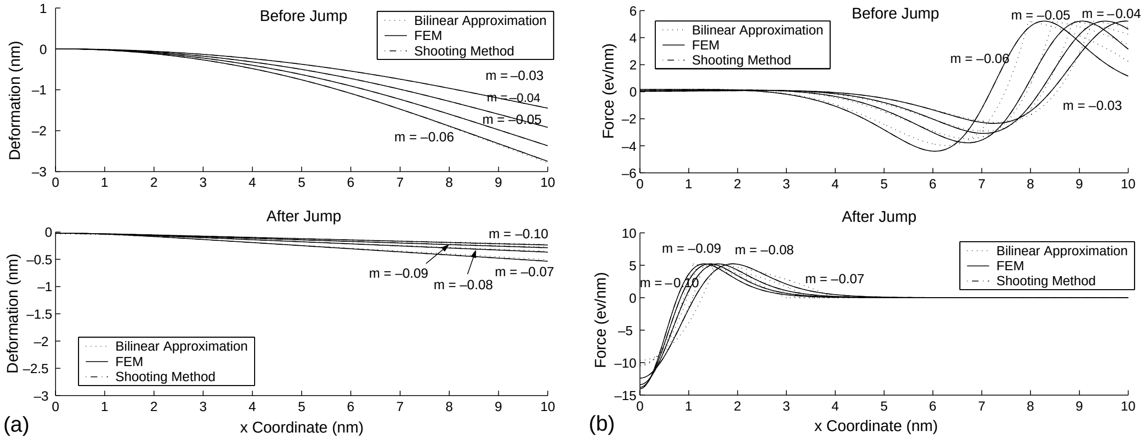

Fig. 4. Bilinear approximation, FEM, and shooting method solutions for nanobeam with $2L = 20$ nm and $d = 0.40$ nm and different substrate curvatures before and after the jump: (a) deformation; (b) van der Waals forces.

herein. Fig. 4(a) shows the change in deformation of the nanobeam as the curvature of the substrate changes from -0.03 to -0.1 nm^{-1}. Up to $m = -0.06$ nm^{-1} the curvatures of the substrate and the beam are nearly the same with small relative deformation; the corresponding van der Waals forces are shown in Fig. 4(b). However, when the curvature changes to -0.07 nm^{-1} the relative deformation increases significantly and the curvature of the beam decreases; the corresponding van dan Waals forces distribution is shown in Fig. 4(b). Hence the critical curvature is -0.06 nm^{-1} at which the jump phenomenon occurs for this case.

Figs. 5 and 6 show deformations of nanobeams with the same diameter but different lengths. In Fig. 5 the change of curvature of the substrate from -0.01 to -0.012 nm^{-1} produces the jump phenomenon. From Fig. 6(a) it can be seen that the deformed nanobeam has the same curvature as the substrate before the critical curvature of -0.01 nm^{-1} for this case. Beyond the critical curvature of the substrate, the nanobeam deforms significantly and the curvature of the beam reduces. In Fig. 6(a) the deformation of the substrate and the curvature of the substrate are apart by r_0, which is so small compared to the deformation of the nanobeam that the nanobeam seems to be coincident with the substrate.

Fig. 7 shows further details of the behavior of nanobeam shown in Figs. 5 and 6. From Fig. 7(d), it can be observed that the van der Waals forces shift from the right side of the nanobeam to the left side of the nanobeam when m changes from -0.01 to -0.0106 nm^{-1}. During this shift, the distribution of the van der Waals forces nearly remains unchanged, the relative deformation of the nanobeam increases significantly and the curvature of the beam reduces, as shown in Fig. 7(c). When m reaches -0.0108 nm^{-1}, the distribution of the van der Waals forces changes and the curvature of the nanobeam becomes very small. From the results in Fig. 7 it is evident that the critical curvature, m_{cr}, for nanobeam with the same diameter is -0.01 nm^{-1} regardless of their lengths.

Next, the effect of diameter is evaluated holding length constant ($2L = 200$ nm). Based on a series of simulations using FEM, for nanobeams with different diameters, but with same length, and different absolute minimum energy U_0 (see Fig. 3), the computed m_{cr} in the nonlinear case is shown in Table 1. It should be noted that m^* in Eq. (10) is calculated using linear approximation of the van der Waals forcing function; whereas, the exact nonlinear van der Waals forcing function as defined in Eq. (3) is used to estimate m_{cr} in Table 1. From Table 1, it can be seen that the absolute value of m_{cr} decreases as the diameter of the nanobeam increases. For nanobeams with the same diameter, the absolute value of m_{cr} increases with the increase in the absolute minimum energy U_0.

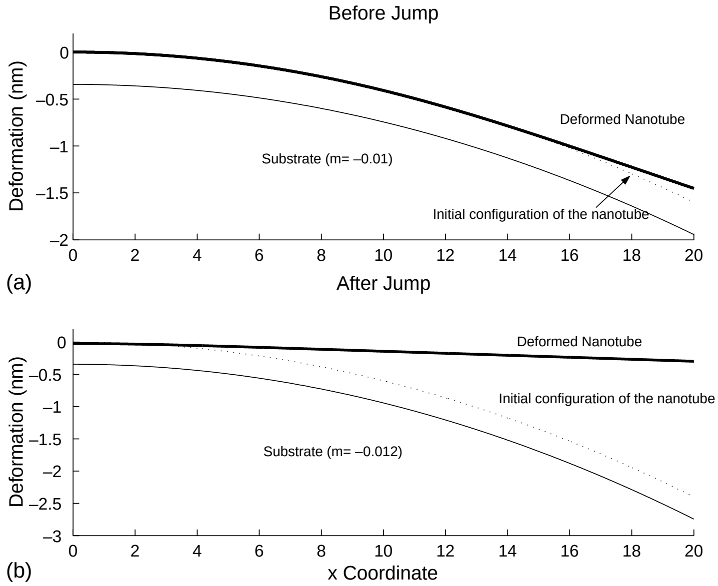

Fig. 5. The deformation of the nanobeam for $2L = 40$ nm and $d = 1.40$ nm (a) before jump, (b) after jump.

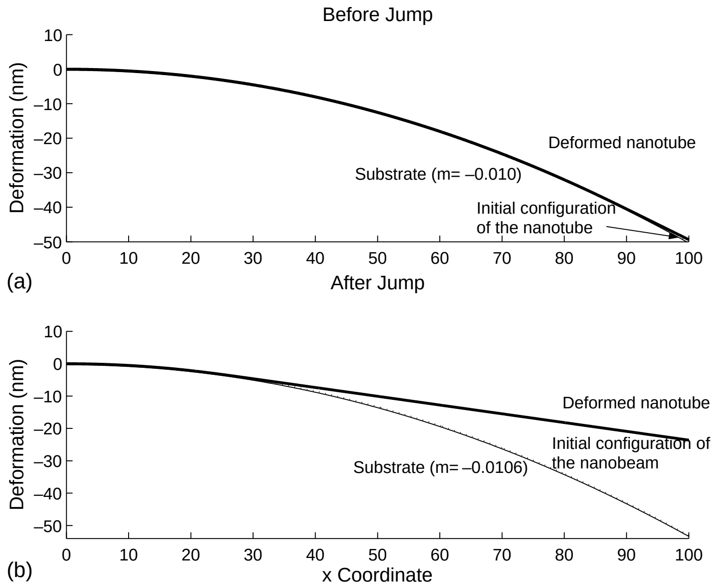

Fig. 6. The deformation of the nanobeam for $2L = 200$ nm and $d = 1.40$ nm (a) before jump, (b) after jump.

Next, an attempt is made to establish an analytical expression for computation of the critical curvature in the nonlinear case. For linear approximation of van der Waals forcing function, it is shown that m^* is proportional to $\sqrt{\frac{2|U_{\mathrm{Lin}}(0)|}{EI}}$ (see Eqs. (10) and (11)). Using a similar approach to establish m_{cr} in nonlinear

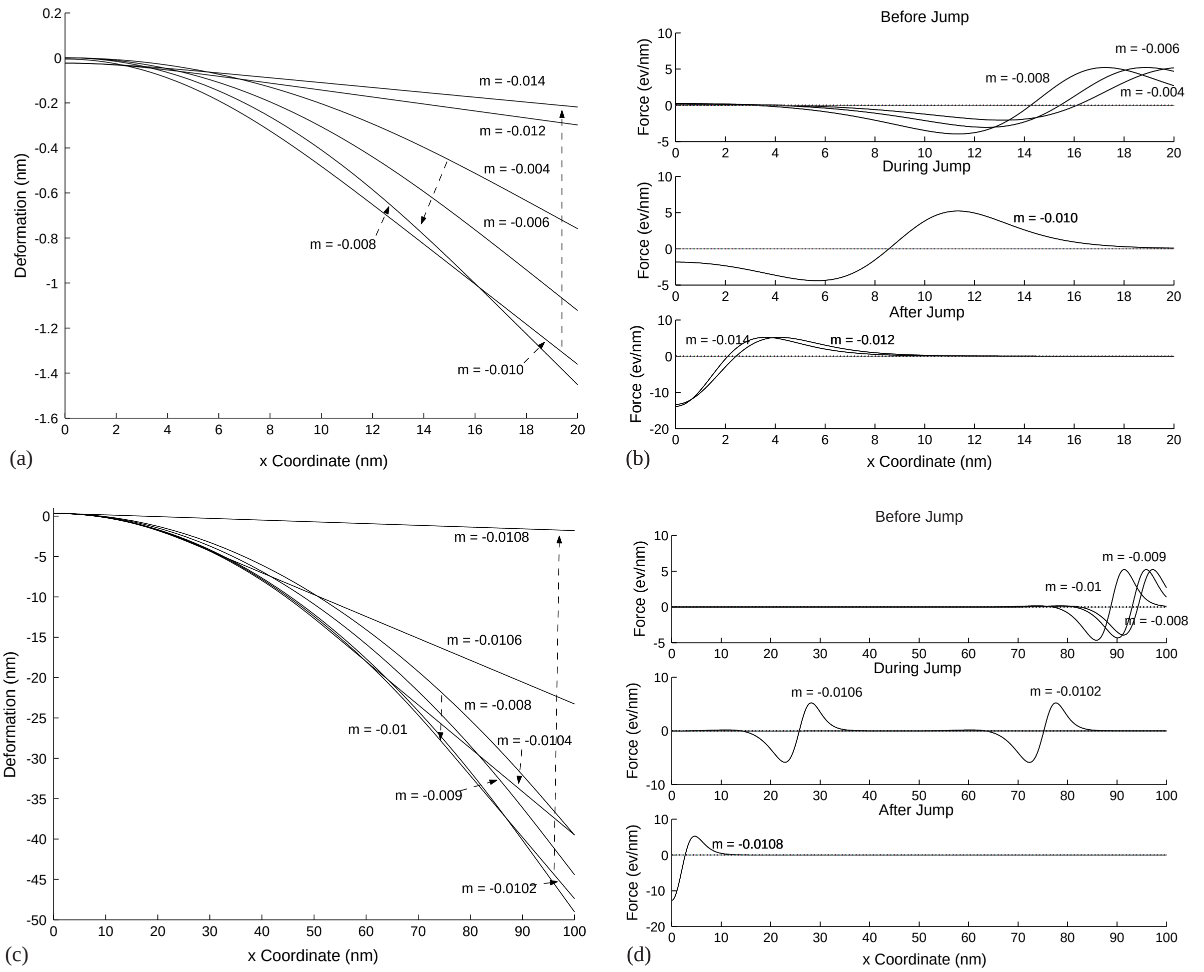

Fig. 7. FEM solutions for the nanobeam with different length and the beam diameter $d = 1.40$ nm: (a) deformation for $2L = 40$ nm; (b) van der Waals forces for $2L = 40$ nm; (c) deformation for $2L = 200$ nm; (d) van der Waals forces for $2L = 200$ nm.

Table 1
m_{cr} (nm^{-1}) for different diameters d and absolute minimum energy U_0

d (nm)	U_0 (eV/nm)			
	0.9516	1.9032	2.8548	3.8046
1.4	−0.0100	−0.0141	−0.0174	−0.0202
2.1	−0.0054	−0.0078	−0.0094	−0.0101
2.8	−0.0036	−0.0050	−0.0062	−0.0070
3.5	−0.0024	−0.0036	−0.0042	−0.0050

case using FEM solutions the relation between m_{cr} with $\sqrt{\frac{U_0}{EI}}$ is evaluated in Fig. 8—where U_0 is absolute minimum energy as defined in Fig. 3. The results of FEM simulation shown in Table 1 are used to generate

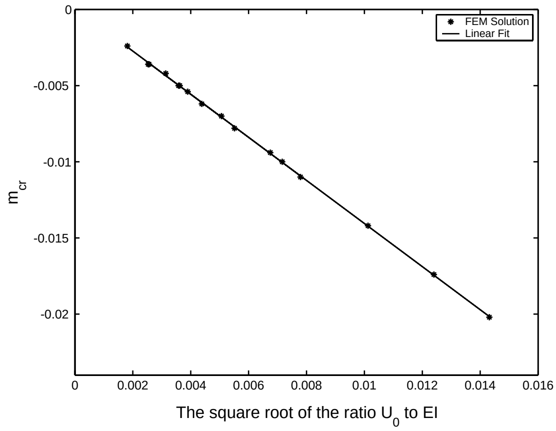

Fig. 8. The relationship between m_{cr} and $\sqrt{\frac{U_0}{EI}}$.

Fig. 8. It is observed that there exists a linear relationship between m_{cr} and $\sqrt{\frac{U_0}{EI}}$ with a slope of −1.414. Hence, the equation for m_{cr} can be written as:

$$m_{cr} = -1.414\sqrt{\frac{U_0}{EI}} \tag{18}$$

Eq. (18) is valid only for the nanobeams having a large aspect ratio. It is important to mention that Eq. (18) is not a general equation for different types of substrate curvatures. It is only valid for the parabolic curvature of the substrate. Also we have not considered large deformation effects; hence the analysis results are applicable for $-2 < m_{cr}L < 0$.

Although analysis above is specifically for a single tube-tube contact, it can be generalized for the case of tube-duplet or tube-triplet contacts which are likely to take place at the tube-bundle interface. The main modification is in the potential energy of interaction as discussed elsewhere (Yakobson and Couchman, 2003, Yakobson and Couchman, 2004), with the doubled or tripled depth U_0 and somewhat extended range (see Fig. 3 in Yakobson and Couchman (2004)).

4. Conclusions

Analytical, finite element and shooting methods have been used to solve the deformation of a nanotube subjected to nonlinear van der Waals forces. All three methods give consistent results. As the critical curvature of the substrate is reached, the relative deformation of the beam increases significantly and the curvature of the beam decreases significantly. The resulting jump phenomenon is a characteristic of the interactions of the nanobeam and the van der Waals forcing function. Considering only parabolic curvatures of the substrate for shallow nanotube, it is shown that the critical curvature depends on the bending stiffness of the nanobeam as well as the absolute minimum energy U_0, but does not depend on the length of the nanobeam when the aspect ratio is large. It is shown that in limited cases the critical curvature can be estimated. Deformations of nanotubes are quite different before and after jump phenomenon and could be the reason for the irregularities in the electronic transportation properties of the nanotube observed as the mechanical deformations such as stretching, bending, twisting or flattening occur in carbon nanotube bundles. The results of this study may be applicable to composites of nanotubes where separation phenomenon is suspected to occur.

Acknowledgements

The authors wish to acknowledge the support of the Texas Institute for the Intelligent Bio-Nano Materials and Structure for Aerospace Vehicles, funded by NASA Cooperative Agreement No. NCC-1-02038.

References

Akita, S., Nakayama, Y., Mizooka, S., Takano, Y., Okawa, T., Miyatake, Y., Yamanaka, S., Tsuji, M., Nosaka, T., 2001. Applied Physics Letter 79, 1691–1693.

Baughman, R.H., Cui, C., Zakhidov, A.A., Lqbal, Z., Barisci, J.N., Spinks, G.M., Wallace, G.G., Mazzoldi, A., Rossi, D.D., Rinzler, A.G., Jaschinski, O., Roth, S., Kertesz, M., 1999. Science 284, 1340–1344.

Collins, P.G., Bradley, K.B., Ishigami, M., Zettl, A., 2000. Science 287, 1801–1804.

Dequesnes, M., Rotkin, S.V., Aluru, N.R., 2002. Nanotechnology 13, 120–131.

Hertel, T., Walkup, R.E., Avouris, P., 1998. Physical Review B 58, 13870–13878.

Iijima, S., 1991. Nature 354, 56–58.

Israelachvili, J., 1992. Intermolecular and Surface Forces, Academic Press, second ed.

Kudin, K.N., Scuseria, G.E., Yakobson, B.I., 2001. Physical Review B 64, 235406/10.

Peng, S., Cho, K., 2000. Nanotechnology 11, 57–60.

Yakobson, B.I., Couchman, L.S., 2003. Persistence length and nanomechanics of random coils and bundles nanotubes, submitted for publication.

Yakobson, B.I., Couchman, L.S., 2004. Carbon nanotubes: supramolecular mechanics. In: Schwartz, J.A. et al. (Eds.), Encyclopedia of Nanoscience and Nanotechnology. Marcel Dekker, New York, DOI: 10.1081/E-ENN 120009130.